Biophysical Chemistry 171 (2013) 9–15

Contents lists available at SciVerse ScienceDirect

Biophysical Chemistry

journal homepage: http://www.elsevier.com/locate/biophyschem

Structure and effect of sarcosine on water and urea by using molecular dynamics simulations: Implications in protein stabilization

Narendra Kumar, Nand Kishore *

Department of Chemistry, Indian Institute of Technology Bombay, Powai, Mumbai 400076, India

HIGHLIGHTS

- MD simulations of sarcosine have been performed in water and in water + urea system.
- RDFs and SDFs were examined along with hydrogen bond dynamics.
- Results support indirect mechanism of protein stabilization.
- Sarcosine counteracts urea by increasing its solvation.

GRAPHICAL ABSTRACT

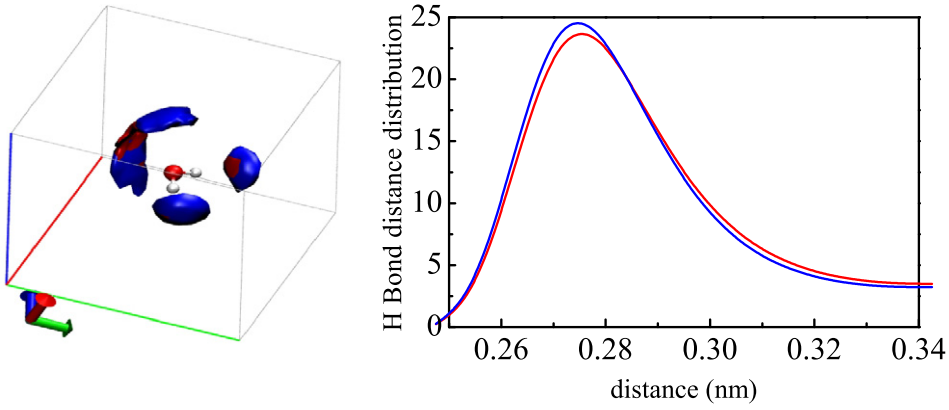

ARTICLE INFO

Article history:
Received 5 October 2012
Received in revised form 30 October 2012
Accepted 13 November 2012
Available online 4 December 2012

Keywords:
Sarcosine
Urea
Molecular dynamics simulation
Radial distribution function
Hydrogen bond dynamics
Diffusion constant

ABSTRACT

Sarcosine is one of the most important protecting osmolytes which is also known to counteract the denaturing effect of urea. We used molecular dynamics simulation methods to investigate the mechanism of protein stabilization and counteraction of urea by sarcosine. We found that sarcosine enhanced the tetrahedral structure of water and strengthened its hydrogen bonding network. We also found that sarcosine did not form clusters unlike glycine. Our results show strong interaction between sarcosine and urea molecules. Addition of sarcosine enhanced the urea–water structure and urea–water lifetime indicated an increase in the solvation of urea. These findings suggest that sarcosine indirectly stabilizes protein by enhancing water–water structure thus decreasing the hydrophobic effect and counteracts the effect of urea by increasing the solvation of urea and directly interacting with it leaving urea less available to interact with protein.

1. Introduction

Osmolytes are naturally occurring organic molecules which are known to affect the conformational stability of proteins. Depending on their effect on protein stability, osmolytes are categorized in two types: protective or stabilizing osmolytes and destabilizing or denaturing osmolytes [1,2]. Methylamines, amino acids, and polyols belong to stabilizing, whereas urea is in the destabilizing category of naturally occurring osmolytes [3–5]. Osmolytes such as trimethylamide-N-oxide (TMAO), sarcosine (N-methylglycine), glycine betaine, and glycerophosphocholine are known to, despite stabilizing proteins,

* Corresponding author.
E-mail address: nandk@chem.iitb.ac.in (N. Kishore).

0301-4622/$ – see front matter © 2012 Elsevier B.V. All rights reserved.
http://dx.doi.org/10.1016/j.bpc.2012.11.004

counteract the denaturing effect of urea which has been of long research interest, still much of underlying mechanism remains unknown [3,4,6–13].

Sarcosine is one of the most important protective osmolyte which is known to stabilize proteins as well as counteract the denaturing effect of urea. It is also used in the treatment of Schizophrenia [14] and has recently been shown to act as bio-marker during prostate cancer progression [15]. Although there have been many studies on its affect on the protein stability and on counteraction of denaturing effect of urea [3,4,7,10,12,16,17], the mechanism by which sarcosine stabilizes proteins and counteracts the denaturation of proteins caused by urea is missing.

Holthauzen and Bolen [10] observed that sarcosine and urea act independently on protein as there is no competition between them at the protein surface. A slight synergy was found between sarcosine and urea by using phase diagram method [18] which is also consistent with results by Venkatesu and Lee [8]. They found that, for example, the presence of 1 M sarcosine increased the transition temperature, (T_m), by 4 °C of α-chymotrypsin and the presence of 1 M urea decreased the T_m by 6 °C. However, when protein was taken in 1 M sarcosine + 1 M urea, there was an overall increase of 3 °C in the T_m of the same protein [8]. That means sarcosine acts as stronger osmolyte and urea becomes weaker denaturant which is an indicative of synergy. For TMAO–urea mixtures, a similar situation was found where synergy between TMAO and urea was due to strong hydrogen bonding at TMAO–oxygen, and solvation of TMAO in aqueous urea [19,20]. In aqueous TMAO solution, TMAO interacted with peptide groups by making hydrogen bonds to its hydrated waters, however, in aqueous TMAO–urea solutions, TMAO has an option of interacting with peptide groups through intercalated urea. Therefore, the spacing between TMAO and peptide groups was increased due to the presence of urea or in other words TMAO is more excluded from the protein surface, hence making TMAO a more potent stabilizer [20]. Our results on the methylamine sarcosine are fully consistent with the methylamine TMAO.

This study is an attempt to understand the structure of aqueous sarcosine and its effect on structure and hydrogen bonding network of water which has serious implications on stabilization of proteins [21,22]. We have also studied sarcosine–urea interactions to explore its counteracting mechanism of denaturing effect of urea on proteins.

2. Computational methods

Molecular dynamics simulations were performed for aqueous sarcosine and aqueous sarcosine + urea systems (Table 1). The simulations were carried out using isothermal–isobaric (NPT) ensemble at $T = 298.15$ K and $P = 1$ bar. GROMACS 3.3.1 molecular dynamics simulation package [23,24] was used for all the systems. Periodic boundary conditions and minimum image conventions were applied in all dimensions. The equations of motion were integrated with leap-frog algorithm at a time step of 1 fs. The coordinates were saved at every 100 fs in the production simulations. Berendsen et al.'s coupling algorithm [25] was employed to maintain constant temperature and pressure with time constant of 0.2 ps and pressure relaxation time of 2 ps. Initial configurations for all the simulations were generated using PACKMOL [26]. Steepest descent energy minimization was performed until the maximum force was smaller than 50 kJ mol^{-1} nm^{-1} followed by 7 ns of production run where the last 5 ns of the production run was used for further analysis. Equilibration of the simulations was checked by monitoring potential energy, density and radial distribution functions (RDFs). We found that the densities of sarcosine solutions were in excellent agreement with the experimental values with maximum error of 0.6% [27]. In all the simulations OPLS all-atom force field [28] was used for sarcosine and urea. Water was described by the extended simple point charge (SPC/E) model [29]. Geometry of sarcosine (Fig. 1) was optimized by using HF/6-31G* approach included in Gaussian 03 software [30]. ESP method [31] was used to derive the partial charges in sarcosine. This method was used as it best produced charges for OPLS force field. We used R.E.D. Server [32] to do ESP calculations. In Table S1, the Cartesian coordinates and the partial charges of sarcosine atoms are reported.

The Lennard–Jones (LJ) potential was used to calculate intermolecular interaction energy between pairs of neighboring atoms with cut-off distance of 1.2 nm and short-range columbic interactions were estimated by using point charge columbic interactions with cut-off distance same as LJ potential. The Particle-Mesh Ewald (PMF) electrostatics [33] was used to calculate the long range interactions. Long range dispersion correction was applied for both energy and pressure. LINCS [34] algorithm was applied to constrain all bonds.

Table 1
Overview of the system simulated. *S*, *U* and *W* represent sarcosine, urea and water respectively. N_S, N_U, and N_W represent number of sarcosine, urea, and water molecules present in the system respectively. M_S is the molarity of sarcosine and M_U is the molarity of urea. *V* and *d* represent volume and density of the system.

System	N_S	N_U	N_W	V(nm^3)	d(g cm^{-3})	M_S(M)	M_U(M)
W	0	0	1400	41.92	0.999	0.00	0.00
1S	30	0	1370	44.22	1.027	1.13	0.00
2S	60	0	1340	46.59	1.051	2.14	0.00
3S	90	0	1310	48.98	1.072	3.05	0.00
4S	120	0	1280	51.42	1.090	3.88	0.00
5S	150	0	1250	53.86	1.106	4.62	0.00
6S	180	0	1220	56.33	1.121	5.30	0.00
U	0	280	1120	53.17	1.155	0.00	8.74
U1S	40	290	1070	56.12	1.179	1.18	8.58
U2S	80	300	1020	60.34	1.198	2.20	8.26
U3S	120	310	970	64.00	1.214	3.11	8.04
U4S	160	320	920	67.67	1.228	3.93	7.85

3. Results and Discussion

3.1. Effect of sarcosine on water structure and in its hydrogen bonding dynamics

We investigated the radial distribution function (RDF) between water oxygens to see the influence of sarcosine on water structure. The RDFs between water oxygen in pure water (system W) and in the presence of sarcosine (system 3S and 6S) are given in Fig. 2. We note that addition of sarcosine did not disrupt the tetrahedral structure of water but enhanced the first peak of water oxygen–water oxygen (OW–OW) RDF. To get further insights, we also investigated spatial distribution functions (SDFs) [35,36] of oxygen water with respect to water, displayed as isosurfaces in Fig. 3a–c, including 12% of all the molecules within 1 nm of distance. We observed an increase in the spatial density of water oxygen upon addition of sarcosine indicating the higher population of tetrahedrally oriented waters and strengthening of

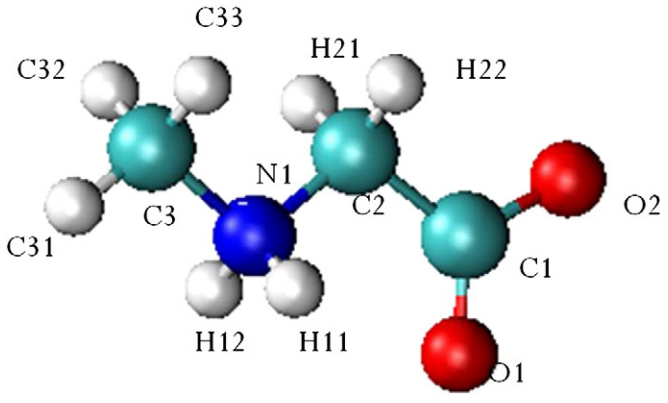

Fig. 1. Structure and labeling scheme of sarcosine.

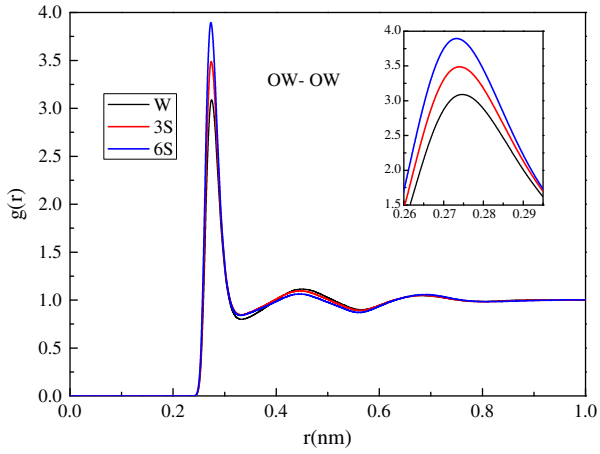

Fig. 2. Water oxygen–water oxygen radial distribution function. OW represents the oxygen of water molecule.

hydrogen bonding network of water. This prompted us to investigate the hydrogen bonding properties of water in different solutions.

A cut-off radius of 0.35 nm between donor and acceptor, and donor–hydrogen–acceptor angle of 35° were taken to define hydrogen bonds. Inspection of donor–hydrogen–acceptor angle and distance distribution between hydrogen bonded water molecules (Fig. 4) reveal that probability distribution increases significantly at the peaks (0.274 nm for hydrogen bond length and 8.9° for angle distribution), and we observe that hydrogen bond angles as well as hydrogen bond distances move to the shorter angles and distances respectively upon the addition of sarcosine, therefore, increasing the ratio of strong hydrogen bonds between water molecules.

3.2. Sarcosine–water interactions

Relevant sarcosine–water RDFs are plotted in Fig. 5a–b. We notice significant increase in the first peak of sarcosine oxygen – water oxygen

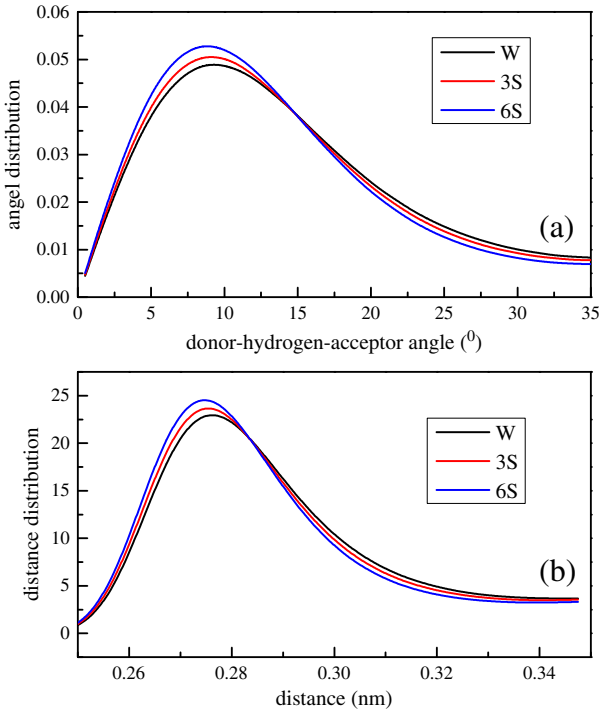

Fig. 4. Hydrogen bond (a) angle and (b) distance distribution between water molecules.

(OS–OW) RDF upon addition of sarcosine indicating strengthening of the sarcosine–water structure which can be attributed to increase in the hydrogen bonding between sarcosine and water, which is clear in hydrogen bond angle and distance distribution (Fig. 5c–d) where hydrogen bond angle and distance moves to shorter angle and distance respectively. In case of sarcosine nitrogen–water oxygen (NS–OW) RDF, second peak is more pronounced than the first peak. Addition of sarcosine has a negligible effect on the first peak of NS–OW RDF indicating that addition of sarcosine has very little effect on hydrogen bonding between

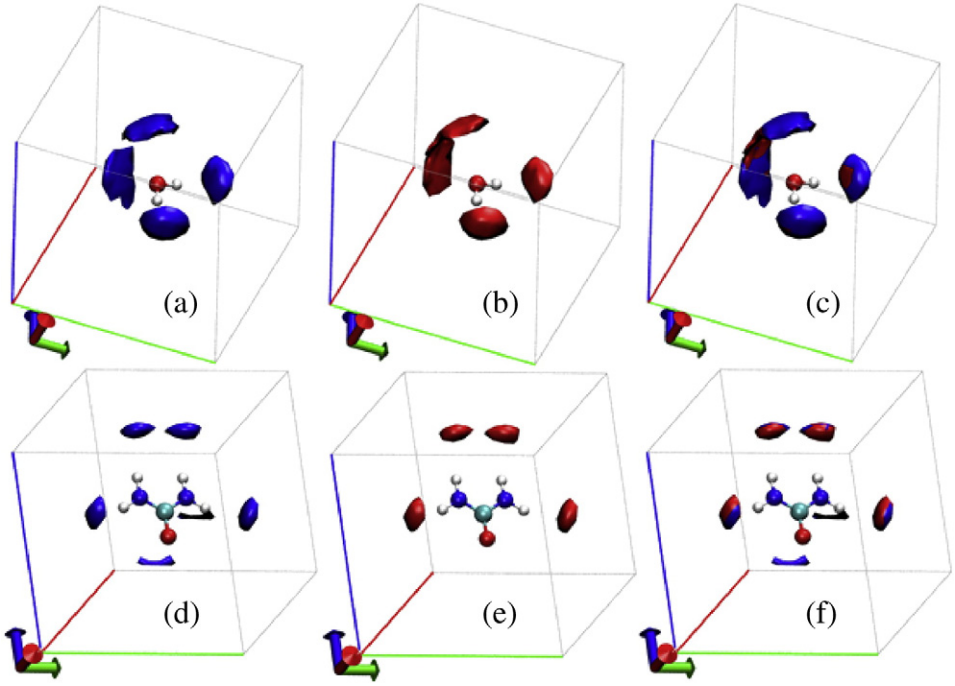

Fig. 3. Spatial distribution functions of water oxygen with respect to (a), (b) and (c) water and (d), (e) and (f) urea. Plot (a) is in pure water (system W, blue), similarly (b) in presence of sarcosine (system 6S, red) and, (c) is combined (a) and (b) plots. Plot (d) in aqueous urea (system U, blue), (e) in presence of aqueous urea + sarcosine (system U4S, red) and, (f) is combined (d) and (e) plots.

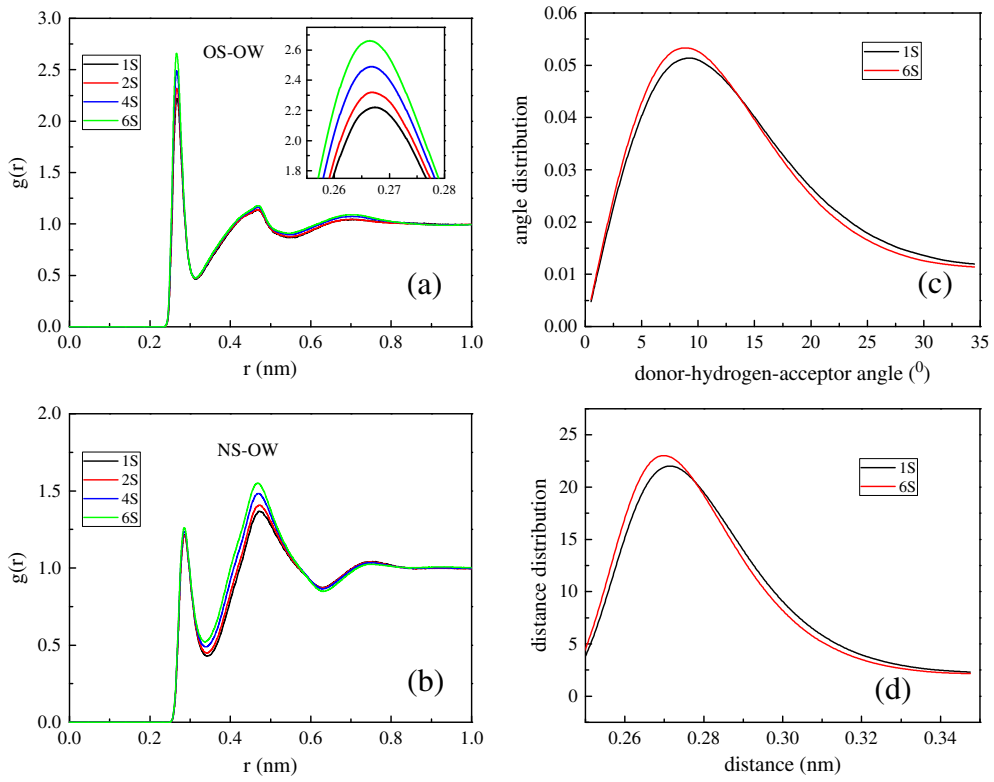

Fig. 5. (a) and (b) Sarcosine–water radial distribution functions and hydrogen bond (c) angle and (d) distance distribution between sarcosine and water. OS and NS are the oxygen and nitrogen atoms of sarcosine.

sarcosine nitrogen and water, but the second peak is enhanced which is likely due to increase in van der Waals interaction between methyl group of sarcosine and water. Therefore, it can be concluded that sarcosine interacts with water by forming hydrogen bonding between oxygen and nitrogen of sarcosine with water where the hydrogen bond between sarcosine oxygen and water is more pronounced than sarcosine nitrogen and water. Sarcosine also interacts with water by van der Waals interactions.

3.3. Structure of sarcosine

The NH2+ and COO− groups of sarcosine can interact with each other through hydrogen bonding, therefore, the relevant RDF between sarcosine nitrogen and sarcosine oxygen (NS–OS) is shown in Fig. 6. The first peak of NS–OS RDF is highly populated than second and third peak indicating sarcosine mostly interact with itself largely by hydrogen bonding. Addition of sarcosine causes a slight decrease in the first peak of NS–OS RDF which is likely due to higher probability of repulsions between COO− and between NH2+ groups than attractions between COO− and NH2+ groups (probability of repulsions is 56% and of attractions is 44%). Sarcosine rather interacts with water and urea (see sarcosine–water and sarcosine–urea RDFs).

Does sarcosine form clusters? Glycine is known to form clusters or aggregates [37,38]. On the other hand, glycine betaine does not form clusters [39]. The structure of sarcosine is analogous to glycine and glycine betaine prompted us to investigate whether sarcosine form clusters as cluster formation can have major consequences in protein stabilization [39,40].

To investigate the cluster formation, we calculated the number of water molecules in the first hydration shell (taken as 0.35 nm) of the sarcosine molecule. Average number of water molecules per sarcosine versus sarcosine concentration is shown in Fig. 7. As sarcosine concentration increases, the number of water molecules decreases uniformly. This uniform decrease is more likely due to random contacts between sarcosine molecules and mutual sharing of hydration shell of individual sarcosine molecules than forming clusters which will become clear below.

To further investigate whether sarcosine forms clusters, we adopted the method used by earlier workers [41–43]. According to this method, the local environment around a molecule can be decided as low, average or high density regions as follows:

low if $n < n_0 - \sigma$

average if $n_0 - \sigma \le n \le n_0 + \sigma$

high if $n \ge n_0 + \sigma$

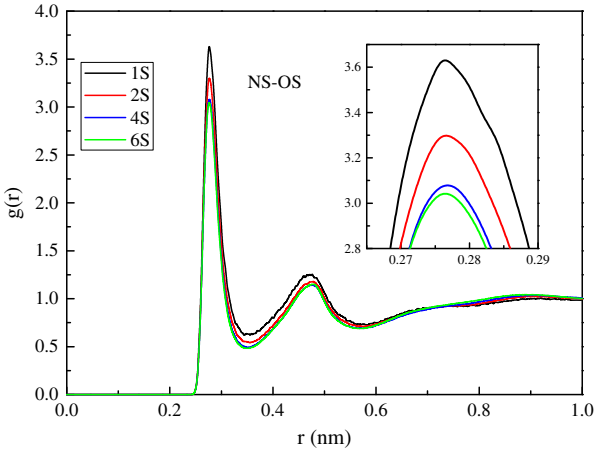

Fig. 6. Sarcosine nitrogen–sarcosine oxygen radial distribution function. Atomic notations are the same as in Fig. 5.

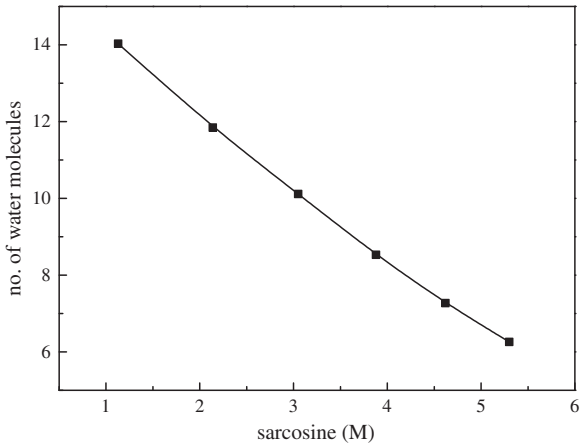

Fig. 7. Average number of water molecules per sarcosine within 0.35 nm from sarcosine atoms.

where n_0 is the average number of solute within a sphere of radius r. n_0 was calculated as $4/3\pi r^3\rho$, where ρ is the bulk number density of solute. n is the number of solute molecules present in the sphere of radius of r around a test solute molecule and σ is the fluctuation which is taken 10% of the n_0 to relax the criteria. The value of r is taken 0.6 nm as, at this value, sarcosine–sarcosine RDF almost becomes 1.

In Table S2, the values of n, n_0, and their difference along with σ are given for all the systems. Here we notice that the value of $n-n_0$ is less or almost equal to σ which is, according to above criteria, has an average density or no formation of sarcosine clusters. And, also increase in the concentration of sarcosine or addition of urea has a negligible effect on local density of sarcosine.

3.4. Effect of sarcosine on urea–urea and urea–water interactions

To see the effect of sarcosine on urea–urea interactions, relevant urea–urea RDFs are calculated. The RDFs for system U and for system U4S are shown in Fig. 8a–c. The RDFs of aqueous urea are in accordance with previous studies [44,45]. Two peaks of urea oxygen–urea oxygen (OU–OU), urea oxygen–urea nitrogen (OU–NU) and three peaks of urea nitrogen–urea nitrogen (NU–NU) RDFs show the association of urea molecule in the form of dimer and trimer [45]. Although addition of sarcosine into urea solution depletes the urea–urea structure, sarcosine does not cause any abrupt change in association properties of urea and it has negligible effect on hydrogen bonding between urea molecules (Fig. 8a). Urea–water RDFs are shown in Fig. 9 for system U and U4S. RDFs for aqueous urea (system U) are similar to previous studies [44,45]. Urea–water RDFs increase significantly upon addition of sarcosine. Sarcosine has major effect on first peak of urea nitrogen–water oxygen (NU–OW) RDF indicating enhancement in hydrogen bonding between urea nitrogen and water, therefore, increasing the solvation of urea i.e. urea will be less available to interact with protein consequently increasing the stability of protein. To see spatial distribution of water around urea molecules, we investigated water oxygen SDF around the center of the mass of urea as displayed in Fig. 3d–f including 38% of all the molecules within 1 nm of distance. We see an increase in the water density around the oxygen and nearby hydrogen atoms of urea molecule and decrease in around other two hydrogen atoms of urea (see Fig. 3d–f). This decrease might be due to hydrogen bonding interactions between sarcosine oxygen and urea hydrogen atoms.

3.5. Sarcosine–urea interactions

RDFs of sarcosine nitrogen–urea oxygen (NS–OU) and sarcosine oxygen–urea nitrogen (OS–NU) (Fig. 10) indicate that sarcosine interacts with urea mostly through hydrogen bonding. Increase in concentration of sarcosine has negligible effect on sarcosine–urea structure with slight increase and decrease in the first peak of RDFs of NS–OU and OS–NU respectively which corresponds to hydrogen bonding.

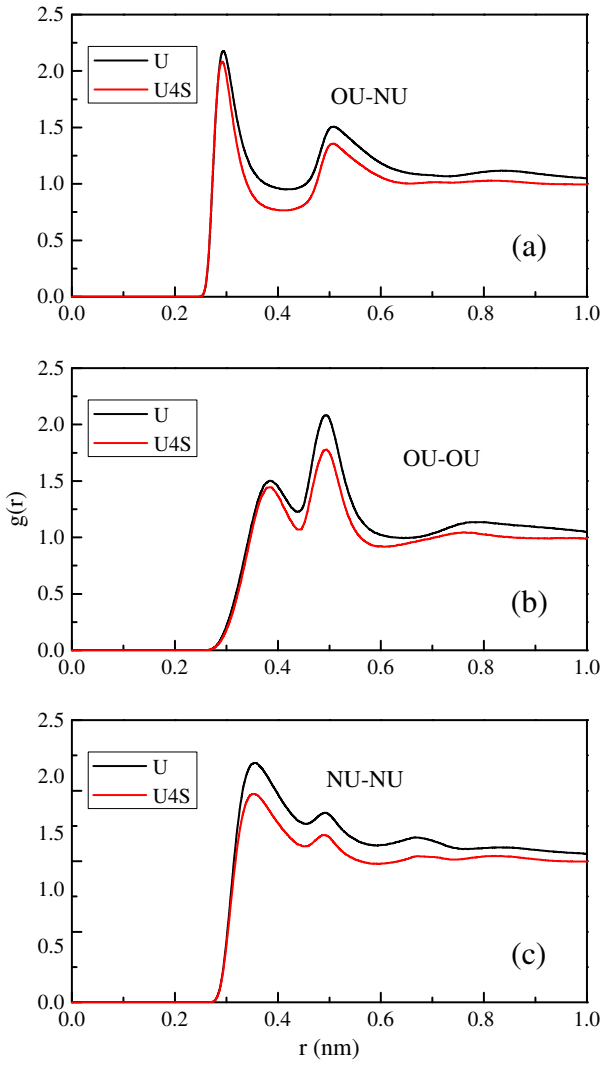

Fig. 8. Urea–urea radial distribution functions between different atoms for the system *U* and *U4S*. NU and OU represent nitrogen and oxygen atoms of urea molecule respectively.

3.6. Hydrogen bond lifetime

We calculated interrupted hydrogen bond lifetime [46,47] to check the stability of hydrogen bonds in sarcosine solutions. To calculate the lifetime, we used the theory of Luzar and Chandler [46] which uses autocorrelation function of hydrogen bonds to analyze the lifetime. Lifetime for pure water in our simulation was found to be 1.56 ps which was higher than the literature value of 1.20 ± 0.08 ps [48]. This difference can be due to the difference in water-model used and hydrogen bonding criteria although the overall effect should not change while comparing with sarcosine (or sarcosine and urea) solutions. The interrupted hydrogen bond lifetimes for all the systems simulated are given in Table 2. Addition of sarcosine increased the water–water and water–sarcosine lifetime significantly. We notice that water–sarcosine hydrogen bond is longer lived than water–water hydrogen bond. On the other hand, addition of 8.74 M urea (system U) increases lifetime only slightly (8%) and water–urea lifetime was ≈60% less than water–water lifetime hence urea has negligible effect on hydrogen bond properties of water which is in accordance with literature [6,45,36]. Urea–water hydrogen bond lifetime increases upon addition of sarcosine which again shows the increase in solvation of urea.

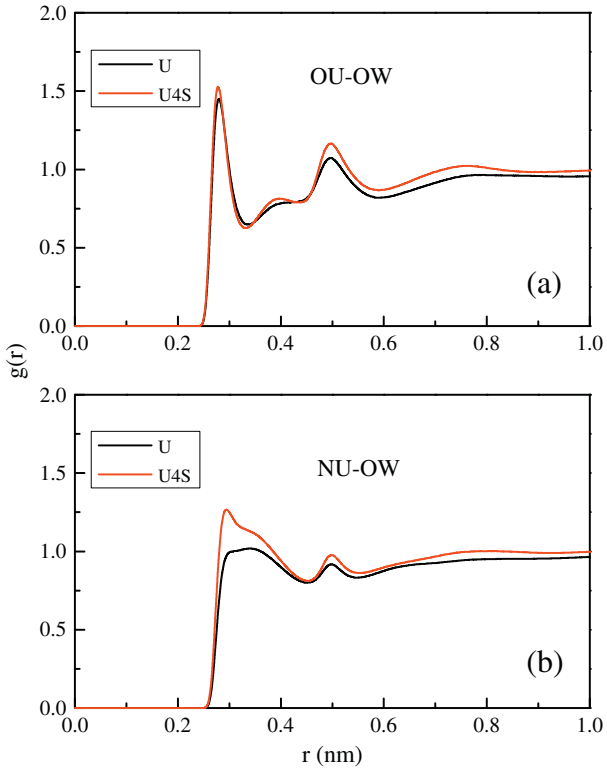

Fig. 9. Urea–water radial distribution functions. Atomic notations are the same as in Figs. 2 and 8.

3.7. Diffusion coefficients

Translational self-diffusion coefficients for pure water, sarcosine and urea were calculated by using famous Einstein relation [49]. The values of diffusion coefficients for some systems are given in Table 3. Diffusion coefficients of pure water (*W*) and urea (*U*) are in excellent agreement with literature value [50,51]. The decrease in the diffusion coefficient of water, sarcosine and urea was found as anticipated after the addition of urea or sarcosine. The decrease in diffusion coefficient of water caused by sarcosine is relatively higher than urea. Diffusion coefficient of urea changes significantly upon addition of sarcosine which is likely to reflect strong interaction between urea and sarcosine.

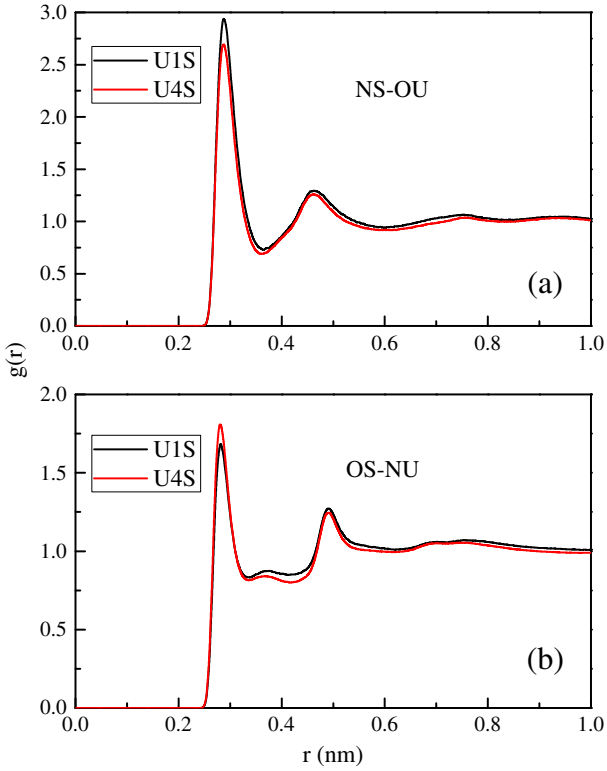

Fig. 10. Sarcosine–urea radial distribution functions. Atomic notations are the same as in Figs. 5 and 8.

Table 2
Lifetime (in ps) of hydrogen bonds formed between different molecules. WW, WS and WU represent water–water, water–sarcosine, and water–urea systems.

Sys.	WW	WS	Sys.	WW	WS	WU
W	1.56					
1S	1.70	2.04	*U*	1.69		0.60
2S	1.92	2.33	*U1S*	1.99	2.78	0.72
3S	2.23	2.63	*U2S*	2.39	3.35	0.93
4S	2.61	3.05	*U3S*	3.04	4.19	1.18
5S	3.13	3.65	*U4S*	3.99	5.70	1.63
6S	3.81	4.45				

4. Summary and conclusions

In this study, we investigate structure and effect of sarcosine on water and urea by taking into account hydrogen bonding, distribution functions and diffusion coefficients to have deeper understanding of protein stabilization and counteraction of denaturing effect of urea by sarcosine. The increase in the first peak of water oxygen–water oxygen RDF in the presence of sarcosine indicated the strengthening of tetrahedral structure as well as hydrogen bonding network of water which becomes clear from shortening of hydrogen bond angle and distance and increase in the lifetime of water molecules. Strong first peak of sarcosine oxygen–water oxygen RDF indicates strong interaction of between sarcosine and water through hydrogen bonding. Hydrogen bond lifetime between sarcosine and water is stronger than water–water and urea–water indicating more involvement of water with sarcosine, in other words, there will be less availability of water to solvate protein backbone, therefore, increasing the protein stability.

Although addition of sarcosine causes decrease in urea structure, sarcosine has a negligible effect on urea–urea hydrogen bonding and it significantly increases the first peak of urea nitrogen–water oxygen RDF showing strong interaction of urea with water through hydrogen bonding. Strong first peak of sarcosine–urea RDFs indicates strong interaction between sarcosine and urea which is supported by a significant decrease in the diffusion coefficient of urea upon the addition of sarcosine. We can, therefore, conclude that sarcosine mostly counteracts the denaturing effect of urea by increasing the solvation of urea and by directly interacting with it leaving urea less available to interact with proteins, in other words, helping proteins to maintain their stability.

Table 3
Self-diffusion coefficients[a] (in $cm^2 s^{-1}$) of water (D_W), sarcosine (D_S) and urea (D_U) for some systems.

System	$D_W \times 10^{-5}$	$D_S \times 10^{-5}$	$D_U \times 10^{-5}$
W	2.62		
1S	2.00	0.65	
4S	1.03	0.26	
6S	0.58	0.17	
U	1.73		0.94
U1S	1.30	0.35	0.56
U3S	0.63	0.14	0.25
U4S	0.40	0.11	0.14

[a] Maximum error in calculating diffusion coefficients is 4%.

Acknowledgment

Computing time from IIT Bombay Computer Center is gratefully acknowledged. N. Kumar acknowledges CSIR, New Delhi for a Junior Research Fellowship.

Appendix A. Supplementary data

Supplementary data to this article can be found online at http://dx.doi.org/10.1016/j.bpc.2012.11.004.

References

[1] P.H. Yancey, M.E. Clark, S.C. Hand, R.D. Bowlus, G.N. Somero, Living with water stress: evolution of osmolyte systems, Science 217 (1982) 1214–1222.
[2] C.Y. Hu, B.M. Pettitt, J. Roesgen, Osmolyte solutions and protein folding, F1000, Biology Reports 1 (2009) 41.
[3] P.H. Yancey, G.N. Somerot, Counteraction of urea destabilization of protein structure by methylamine osmoregulatory compounds of elasmobranch fishes, Biochemical Journal 183 (1979) 317–323.
[4] P.C. Withers, M. Guppy, Do Australian desert frogs co-accumulate counteracting solutes with urea during aestivation? Journal of Experimental Biology 199 (1996) 1809–1816.
[5] G.D. Rose, P.J. Fleming, J.R. Banavar, A. Maritan, A backbone-based theory of protein folding, Proceedings of the National Academy of Sciences 103 (2006) 16623–16633.
[6] Q. Zou, B.J. Bennion, V. Daggett, K.P. Murphy, The molecular mechanism of stabilization of proteins by TMAO and its ability to counteract the effects of urea, Journal of the American Chemical Society 124 (2002) 1192–1202.
[7] L.R. Singh, T. Ali Dar, I. Haque, F. Anjum, A.A. Moosavi-Movahedi, F. Ahmad, Testing the paradigm that the denaturing effect of urea on protein stability is offset by methylamines at the physiological concentration ratio of 2:1 (urea:methylamines), Biochimica et Biophysica Acta 1774 (2007) 1555–1562.
[8] P. Venkatesu, M.-J. Lee, H.-M. Lin, Osmolyte counteracts urea-induced denaturation of r-chymotrypsin, The Journal of Physical Chemistry B 113 (2009) 5327–5338.
[9] F. Meersman, D. Bowron, A.K. Soper, M.H.J. Koch, Counteraction of urea by trimethylamine N-oxide is due to direct interaction, Biophysical Journal 97 (2009) 2559–2566.
[10] L.M.F. Holthauzen, D.W. Bolen, Mixed osmolytes: the degree to which one osmolyte affects the protein stabilizing ability of another, Protein Science 16 (2007) 293–298.
[11] D.W. Bolen, I.V. Baskakov, The osmophobic effect: natural selection of a thermodynamic force in protein folding, Journal of Molecular Biology 310 (2001) 955–963.
[12] G.S. Ratnaparkhi, R. Varadarajan, Osmolytes stabilize ribonuclease S by stabilizing its fragments S protein and S peptide to compact folding-competent states, Journal of Biological Chemistry 276 (2001) 28789–28798.
[13] Y. Maeda, H. Yamada, T. Ueda, T. Imoto, Effect of additives on the renaturation of reduced lysozyme in the presence of 4 M urea, Protein Engineering 9 (1996) 461–465.
[14] H.-Y. Lane, C.-L. Huang, P.-L. Wu, Y.-C. Liu, Y.-C. Chang, P.-Y. Lin, P.-W. Chen, G. Tsai, Glycine transporter I inhibitor, N-methylglycine (sarcosine), added to clozapine for the treatment of schizophrenia, Biological Psychiatry 60 (2006) 645–649.
[15] A. Sreekumar, L.M. Poisson, T.M. Rajendiran, A.P. Khan, Q. Cao, J. Yu, B. Laxman, R. Mehra, R.J. Lonigro, Y. Li, M.K. Nyati, A. Ahsan, S. Kalyana-Sundaram, B. Han, X. Cao, J. Byun, G.S. Omenn, D. Ghosh, S. Pennathur, D.C. Alexander, A. Berger, J.R. Shuster, J.T. Wei, S. Varambally, C. Beecher, A.M. Chinnaiyan, Metabolomic profiles delineate potential role for sarcosine in prostate cancer progression, Nature 457 (2009) 910–915.
[16] L.M.F. Holthauzen, J. Rösgen, D.W. Bolen, Hydrogen bonding progressively strengthens upon transfer of the protein urea-denatured state to water and protecting osmolytes, Biochemistry 49 (2010) 1310–1318.
[17] M. Auton, D.W. Bolen, J. Rösgen, Structural thermodynamics of protein preferential solvation: osmolyte solvation of proteins, aminoacids, and peptides, Proteins 73 (2008) 802–813.
[18] L.M.F. Holthauzen, M. Auton, M. Sinev, J. Rösgen, Protein stability in the presence of cosolutes, Methods in Enzymology 492 (2011) 61–125.
[19] C.C. Mello, D. Barrick, Measuring the stability of partly folded proteins using TMAO, Protein Science 12 (2003) 1522–1529.
[20] J. Rösgen, R. Jackson-Atogi, Volume exclusion and H-bonding dominate the thermodynamics and solvation of trimethylamine-N-oxide in aqueous urea, Journal of the American Chemical Society 134 (2012) 3590–3597.
[21] B.J. Bennion, V. Daggett, The molecular basis for the chemical denaturation of proteins by urea, Proceedings of the National Academy of Sciences 100 (2003) 5142–5147.
[22] B.J. Bennion, V. Daggett, Counteraction of urea-induced protein denaturation by trimethylamine N-oxide: a chemical chaperone at atomic resolution, Proceedings of the National Academy of Sciences 101 (2004) 6433–6438.
[23] E. Lindahl, B.B. Hess, D. van der Spoel, Gromacs 3.0: a package for molecular simulation and trajectory analysis, Journal of Molecular Modeling 7 (2001) 306–317.
[24] H.J.C. Berendsen, D. van der Spoel, R. van Drunen, Gromacs: a message-passing parallel molecular dynamics implementation, Computer Physics Communications 91 (1995) 43–56.
[25] H.J.C. Berendsen, J.P.M. Postma, W.F. van Gunsteren, A. DiNola, J.R. Haak, Molecular dynamics with coupling to an external bath, Journal of Chemical Physics 81 (1984) 3684–3690.
[26] L. Martínez, R. Andrade, E.G. Birgin, J.M. Martínez, Packmol: a package for building initial configurations, Journal of Computational Chemistry 30 (2009) 2157–2164.
[27] P. Venkatesu, M.-J. Lee, H.-M. Lin, Thermodynamic characterization of the osmolyte effect on protein stability and the effect of GdnHCl on the protein denatured state, The Journal of Physical Chemistry B 111 (2007) 9045–9056.
[28] K. Kahn, T.C. Bruice, Parameterization of OPLS-AA force field for the conformational analysis of macrocyclic polyketides, Journal of Computational Chemistry 23 (2002) 977–996.
[29] H.J.C. Berendsen, J.R. Grigera, T.P. Straatsma, The missing term in effective pair potentials, Journal of Physical Chemistry 91 (1987) 6269–6271.
[30] M.J. Frisch, G.W. Trucks, H.B. Schlegel, G.E. Scuseria, M.A. Robb, J.R. Cheeseman, J.A. Montgomery Jr., T. Vreven, K.N. Kudin, J.C. Burant, J.M. Millam, S.S. Iyengar, J. Tomasi, V. Barone, B. Mennucci, M. Cossi, G. Scalmani, N. Rega, G.A. Petersson, H. Nakatsuji, M. Hada, M. Ehara, K. Toyota, R. Fukuda, J. Hasegawa, M. Ishida, T. Nakajima, Y. Honda, O. Kitao, H. Nakai, M. Klene, X. Li, J.E. Knox, H.P. Hratchian, J.B. Cross, V. Bakken, C. Adamo, J. Jaramillo, R. Gomperts, R.E. Stratmann, O. Yazyev, A.J. Austin, R. Cammi, C. Pomelli, J.W. Ochterski, P.Y. Ayala, K. Morokuma, G.A. Voth, P. Salvador, J.J. Dannenberg, V.G. Zakrzewski, S. Dapprich, A.D. Daniels, M.C. Strain, O. Farkas, D.K. Malick, A.D. Rabuck, K. Raghavachari, J.B. Foresman, J.V. Ortiz, Q. Cui, A.G. Baboul, S. Clifford, J. Cioslowski, B.B. Stefanov, G. Liu, A. Liashenko, P. Piskorz, I. Komaromi, R.L. Martin, D.J. Fox, T. Keith, M.A. Al-Laham, C.Y. Peng, A. Nanayakkara, M. Challacombe, P.M.W. Gill, B. Johnson, W. Chen, M.W. Wong, C. Gonzalez, J.A. Pople, Gaussian 03, Revision C.02, 2004, Gaussian, Inc., Wallingford, CT, 2004.
[31] U.C. Singh, P.A. Kollman, An approach to computing electrostatic charges for molecules, Journal of Computational Chemistry 5 (1984) 129–145.
[32] E. Vanquelef, S. Simon, G. Marquant, E. Garcia, G. Klimerak, J.C. Delepine, P. Cieplak, F.-Y. Dupradeau, R.E.D. Server: a web service for deriving RESP and ESP charges and building force field libraries for new molecules and molecular fragments, Nucleic Acids Research 39 (2011) W511–W517.
[33] U. Essmann, L. Perera, M.L. Berkowitz, T. Darden, H. Lee, L.G. Pedersen, A smooth particle mesh Ewald method, Journal of Chemical Physics 103 (1995) 8577–8593.
[34] B. Hess, H. Bekker, H.J.C. Berendsen, J.G.E.M. Fraaije, LINCS: a linear constraint solver for molecular simulations, Journal of Computational Chemistry 18 (1997) 1463–1472.
[35] A. Vishnyakov, A.P. Lyubartsev, A. Laaksonen, Molecular dynamics simulations of dimethyl sulfoxide and dimethyl sulfoxide–water mixture, Journal of Physical Chemistry A 105 (2001) 1702–1710.
[36] M.C. Stumpe, H. Grubmüller, Aqueous urea solutions: structure, energetics, and urea aggregation, The Journal of Physical Chemistry B 111 (2007) 6220–6228.
[37] S. Hamad, C.E. Hughes, C.R.A. Catlow, K.D.M. Harris, Clustering of glycine molecules in aqueous solution studied by molecular dynamics simulation, The Journal of Physical Chemistry B 112 (2008) 7280–7288.
[38] A. White, S. Jiang, Local and bulk hydration of zwitterionic glycine and its analogues through molecular simulations, The Journal of Physical Chemistry B 115 (2011) 660–667.
[39] A. Fornili, M. Civera, M. Sironi, S.L. Fornili, Molecular dynamics simulation of aqueous solutions of trimethylamine-N-oxide and tert-butyl alcohol, Physical Chemistry Chemical Physics 5 (2003) 4905–4910.
[40] D. Shukla, B.L. Trout, Interaction of arginine with proteins and the mechanism by which it inhibits aggregation, The Journal of Physical Chemistry B 114 (2010) 13426–13438.
[41] H.L. Martinez, R. Ravi, S.C. Tucker, Characterization of solvent clusters in a supercritical Lennard–Jones fluid, Journal of Chemical Physics 104 (1996) 1067–1080.
[42] H. Kokubo, B.M. Pettitt, Preferential solvation in urea solutions at different concentrations: properties from simulation studies, The Journal of Physical Chemistry B 111 (2007) 5233–5242.
[43] R. Sarma, S. Paul, Hydrophobic interactions in presence of osmolytes urea and trimethylamine-N-oxide, Journal of Chemical Physics 135 (2011) 174501–174513.
[44] S. Paul, G.N. Patey, Structure and interaction in aqueous urea-trimethylamine-N-oxide solutions, Journal of the American Chemical Society 129 (2007) 4476–4482.
[45] R.D. Mountain, D. Thirumalai, Importance of excluded volume on the solvation of urea in water, The Journal of Physical Chemistry B 108 (2004) 6826–6831.
[46] A. Luzar, D. Chandler, Hydrogen-bond kinetics in liquid, Nature 379 (1996) 55–57.
[47] D. van der Spoel, P.J. van Maaren, P. Larsson, N. Timneanu, Thermodynamics of hydrogen bonding in hydrophilic and hydrophobic media, The Journal of Physical Chemistry B 110 (2006) 4393–4398.
[48] A. Luzar, D. Chandler, Structure and hydrogen bond dynamics mixtures by computer simulations of water-dimethyl sulfoxide, Journal of Chemical Physics 98 (1993) 8160–8173.
[49] M.P. Allen, D.J. Tildesley, Computer Simulation of Liquids, Oxford Science, Oxford, 1987.
[50] P. Mark, L. Nilsson, Structure and dynamics of the TIP3P, SPC, and SPC/E water models at 298 K, Journal of Physical Chemistry A 105 (2001) 9954–9960.
[51] A. Chandra, T. Ichiye, Dynamical properties of the soft sticky dipole model of water: molecular dynamics simulations, Journal of Chemical Physics 111 (1999) 2701–2709.